Numerical Methods and Analysis for Computing Forward and Inverse Laplace Transform For discrete and continuous signals

Yueyang Shen[1,3], Yupeng Zhang[1,2], Ivo Dinov[1,3]

[1]Statistical Online Computational Resources (SOCR), University of Michigan
[2]Department of Mathematics, University of Wisconsin
[3]Department of Computational Medicine and Bioinformatics, University of Michigan
*To appear on arxiv on April 27th (Updated link will be attached to the updated slides on SOCR website)

April 26, 2023

Overview

Spacekime Analytics - Complex Time Motivations

1. Physics aspect :
   - Different quantum predictions of $\mathbb{R}$ and $\mathbb{C}$ quantum theories[1].

[1] Marc-Olivier Renou et al. "Quantum theory based on real numbers can be experimentally falsified". In: *Nature* 600.7890 (2021), pp. 625–629

[2] Edward Anderson. "Problem of time in quantum gravity". In: *Annalen der Physik* 524.12 (2012), pp. 757–786

Spacekime Analytics - Complex Time Motivations

1. Physics aspect :
   - Different quantum predictions of $\mathbb{R}$ and $\mathbb{C}$ quantum theories[1].
   - Problem with time[2].

[1] Marc-Olivier Renou et al. "Quantum theory based on real numbers can be experimentally falsified". In: *Nature* 600.7890 (2021), pp. 625–629

[2] Edward Anderson. "Problem of time in quantum gravity". In: *Annalen der Physik* 524.12 (2012), pp. 757–786

Spacekime Analytics - Complex Time Motivations

1. Physics aspect :
   - Different quantum predictions of $\mathbb{R}$ and $\mathbb{C}$ quantum theories[1].
   - Problem with time[2].
2. Mathematical aspect: Additional examples
   - The time domain $(\mathbb{R}^+)$ is not a complete algebraic field $(+, *)$:
     - Additive unity (0), element additive inverse (t) : $t + (t) = 0$; is outside $\mathbb{R}^+$ (time-domain).
     - $x^2 + 1 = 0$ has no solutions in time (or in $\mathbb{R}$)

[1] Marc-Olivier Renou et al. "Quantum theory based on real numbers can be experimentally falsified". In: *Nature* 600.7890 (2021), pp. 625–629

[2] Edward Anderson. "Problem of time in quantum gravity". In: *Annalen der Physik* 524.12 (2012), pp. 757–786

Spacekime Analytics - Complex Time Motivations

1. Physics aspect :
   - Different quantum predictions of $\mathbb{R}$ and $\mathbb{C}$ quantum theories[1].
   - Problem with time[2].
2. Mathematical aspect: Additional examples
   - The time domain $(\mathbb{R}^+)$ is not a complete algebraic field $(+, *)$:
     - Additive unity (0), element additive inverse (t) : $t + (t) = 0$; is outside $\mathbb{R}^+$ (time-domain).
     - $x^2 + 1 = 0$ has no solutions in time (or in $\mathbb{R}$)
   - Time forms a subgroup of the multiplicative group of the reals whereas kime $(\mathbb{C})$ is an algebraically **closed** prime field that naturally extends time. (Closure implies universal properties)

[1] Marc-Olivier Renou et al. "Quantum theory based on real numbers can be experimentally falsified". In: *Nature* 600.7890 (2021), pp. 625–629

[2] Edward Anderson. "Problem of time in quantum gravity". In: *Annalen der Physik* 524.12 (2012), pp. 757–786

Spacekime Analytics - Complex Time Motivations

1. Physics aspect :
   - Different quantum predictions of $\mathbb{R}$ and $\mathbb{C}$ quantum theories[1].
   - Problem with time[2].
2. Mathematical aspect: Additional examples
   - The time domain ($\mathbb{R}^+$) is not a complete algebraic field $(+, *)$:
     - Additive unity (0), element additive inverse (t) : $t + (t) = 0$; is outside $\mathbb{R}^+$ (time-domain).
     - $x^2 + 1 = 0$ has no solutions in time (or in $\mathbb{R}$)
   - Time forms a subgroup of the multiplicative group of the reals whereas kime ($\mathbb{C}$) is an algebraically **closed** prime field that naturally extends time. (Closure implies universal properties)
3. Data science aspect: Tensor modeling, random IID sampling, Bayesian interpretation.
   - We study specifically the problem of representing time-series as kime-surfaces .

[1] Marc-Olivier Renou et al. "Quantum theory based on real numbers can be experimentally falsified". In: *Nature* 600.7890 (2021), pp. 625–629

[2] Edward Anderson. "Problem of time in quantum gravity". In: *Annalen der Physik* 524.12 (2012), pp. 757–786

Spacekime Analytics - Complex Time Motivations

1. Physics aspect :
   - Different quantum predictions of $\mathbb{R}$ and $\mathbb{C}$ quantum theories[1].
   - Problem with time[2].
2. Mathematical aspect: ⏩ Additional examples
   - The time domain $(\mathbb{R}^+)$ is not a complete algebraic field $(+, *)$:
     - Additive unity (0), element additive inverse $(t) : t + (t) = 0$; is outside $\mathbb{R}^+$ (time-domain).
     - $x^2 + 1 = 0$ has no solutions in time (or in $\mathbb{R}$)
   - Time forms a subgroup of the multiplicative group of the reals whereas kime ($\mathbb{C}$) is an algebraically **closed** prime field that naturally extends time. (Closure implies universal properties)
3. Data science aspect: Tensor modeling, random IID sampling, Bayesian interpretation.
   - We study specifically the problem of representing time-series as kime-surfaces .

   $\hookrightarrow$ We argue that encoding 1D signal to 2D (images) is natural to human experience: one can generate a 2D/3D scene from a 1D music signal; or for example generating images from text prompts.

[1] Marc-Olivier Renou et al. "Quantum theory based on real numbers can be experimentally falsified". In: *Nature* 600.7890 (2021), pp. 625–629

[2] Edward Anderson. "Problem of time in quantum gravity". In: *Annalen der Physik* 524.12 (2012), pp. 757–786

Approach to represent time series as kime surfaces

Essential Components of Kime surface

1. Analyticity -Sampling, convergent Taylor series (Our work)

Approach to represent time series as kime surfaces

Essential Components of Kime surface

1. Analyticity -Sampling, convergent Taylor series (Our work)
2. Poles of simple singularities (efficiently encoded in Padé approximants)

$$\frac{P(z)}{Q(z)} = \frac{a_0 + a_1 z + ... + a_m z^m}{1 + b_1 z + ... + b_n z^n} \tag{1}$$

3. Branchpoints(Conformally mapped to a disk and then perform Padé 2208.02410.).
4. Essential Singularities.

Approach to represent time series as kime surfaces

Essential Components of Kime surface

1. Analyticity -Sampling, convergent Taylor series (Our work)
2. Poles of simple singularities (efficiently encoded in Padé approximants)

$$\frac{P(z)}{Q(z)} = \frac{a_0 + a_1 z + ... + a_m z^m}{1 + b_1 z + ... + b_n z^n} \tag{1}$$

3. Branchpoints(Conformally mapped to a disk and then perform Padé 2208.02410.).
4. Essential Singularities.

▶ For most data applications, we don't need rigor and techniques to cope with singularity, but in many physical applications, especially in computing and regularizing path integral

Approach to represent time series as kime surfaces

Essential Components of Kime surface

1. Analyticity -Sampling, convergent Taylor series (Our work)
2. Poles of simple singularities (efficiently encoded in Padé approximants)

$$\frac{P(z)}{Q(z)} = \frac{a_0 + a_1 z + ... + a_m z^m}{1 + b_1 z + ... + b_n z^n} \tag{1}$$

3. Branchpoints(Conformally mapped to a disk and then perform Padé 2208.02410.).
4. Essential Singularities.

▶ For most data applications, we don't need rigor and techniques to cope with singularity, but in many physical applications, especially in computing and regularizing path integral

$$\int \mathcal{D}x(t) \exp\left(\frac{i}{\hbar} S[x(t)]\right) \tag{2}$$

spurious singularities emerges and treatment is needed for a renormalizable theory and hence we need to decode information from these features.

Representing time series and kime surfaces - Properties

Concrete examples Closure$\Longrightarrow$Universality

We want a desirable pipeline to implement the process of representing time series and kime surfaces but also to be able to go backwards.

$$f(t) \Longrightarrow F(z) \Longrightarrow f(t) \quad (3)$$

Concrete examples Closure$\Longrightarrow$Universality

We want a desirable pipeline to implement the process of representing time series and kime surfaces but also to be able to go backwards.

$$f(t) \Longrightarrow F(z) \Longrightarrow f(t) \tag{3}$$

Why **Laplace transforms**?

Concrete examples Closure$\Longrightarrow$Universality

We want a desirable pipeline to implement the process of representing time series and kime surfaces but also to be able to go backwards.

$$f(t) \Longrightarrow F(z) \Longrightarrow f(t) \tag{3}$$

Why **Laplace transforms**?

- Laplace transform is useful to analyze Linear Time Invariant systems, which encodes similar information for a observational process when doing **repeated data experiments** at different points anchored at observational time. Furthermore, time translation can be adjusted efficiently

$$\int_0^\infty e^{-st} f(t-a)u(t-a) = e^{-as}F(s) \tag{4}$$

Representing time series and kime surfaces - Properties

Concrete examples Closure $\Longrightarrow$ Universality

We want a desirable pipeline to implement the process of representing time series and kime surfaces but also to be able to go backwards.

$$f(t) \Longrightarrow F(z) \Longrightarrow f(t) \tag{3}$$

Why **Laplace transforms**?

- Laplace transform is useful to analyze Linear Time Invariant systems, which encodes similar information for a observational process when doing **repeated data experiments** at different points anchored at observational time. Furthermore, time translation can be adjusted efficiently

$$\int_0^{\infty} e^{-st} f(t-a)u(t-a) = e^{-as}F(s) \tag{4}$$

- **Probabilistic perspective**, the moment generating function uniquely defines the distribution of a random variable and statistical moments.

Representing time series and kime surfaces - Properties

Concrete examples Closure$\Longrightarrow$Universality

We want a desirable pipeline to implement the process of representing time series and kime surfaces but also to be able to go backwards.

$$f(t) \Longrightarrow F(z) \Longrightarrow f(t) \tag{3}$$

Why **Laplace transforms**?

- Laplace transform is useful to analyze Linear Time Invariant systems, which encodes similar information for a observational process when doing **repeated data experiments** at different points anchored at observational time. Furthermore, time translation can be adjusted efficiently

$$\int_0^\infty e^{-st} f(t-a)u(t-a) = e^{-as}F(s) \tag{4}$$

- **Probabilistic perspective**, the moment generating function uniquely defines the distribution of a random variable and statistical moments.

▶ Other more general way (Embedding time signals as complex Meijer G functions): Meijer G computation. Specifically Meijer G is closed under laplace transform Theoretical Details .(See http://www.socr.umich.edu/TCIU/HTMLs/Chapter4_Laplace_Transform_Meijer_G_Functions.html).

Theorem

Laplace transform is the only transform that satisfies

- *Linearity transform:* $\mathcal{L}[\alpha f + \beta g] = \alpha\mathcal{L}[f] + \beta\mathcal{L}[g]$
- *Algebraic derivatives:* $\mathcal{L}[f'](s) = s\mathcal{L}[f](s) - f(0)$

for analytic functions.

Theorem

The finite Laplace transform $\int_0^{2\pi} f(t)e^{-st}dt$ *is the only transform that satisfies*

- *Linearity transform:* $\mathcal{L}[\alpha f + \beta g] = \alpha\mathcal{L}[f] + \beta\mathcal{L}[g]$
- *Algebraic derivatives:* $\mathcal{L}[f'](s) = s\mathcal{L}[f](s) - f(0) + e^{-2\pi s}f(2\pi)$

- Historically, this algebraic derivative condition was made rigorous from Heaviside operator method on time evolving ODE systems.

Alternative motivations and Examples

1. Differential Equations & Physical Phenomena parallel:
   - Duality between kime complex analytic function and fluid flow:
     - (Cauchy-Riemann) Every complex analytic function gives rise to an incompressible, irrotational, steady fluid flow.
     - Furthermore, for meromorphic functions, the saddles correspond to the saddles in the flow (Analytic function is equivalent to a fluid flow configuration)[3].
2. Invariances:
   - Useful to analyze **Linear Time Invariant** systems under Repeated Experiments situation.
   - Energy invariance:

$$\int_{-\infty}^{\infty} |f(t)e^{-tx}H(t)|^2 dt = \int_{-\infty}^{\infty} |F(x+iy)|^2 dy$$

   Therefore $\|\mathcal{L}f\|_{H^2(\mathbb{C}_+)} = \|f\|_{L^2([0,\infty))}$.
3. Kimesurfaces features visualization examples: ▶ Monotonicity dampens the oscillation in magnitude ▶Periodicity translates to more oscillations on the magnitude

[3] Tyre Newton and Thomas Lofaro. "On using flows to visualize functions of a complex variable". In: *Mathematics Magazine* 69.1 (1996), pp. 28–34

The Laplace transform interface

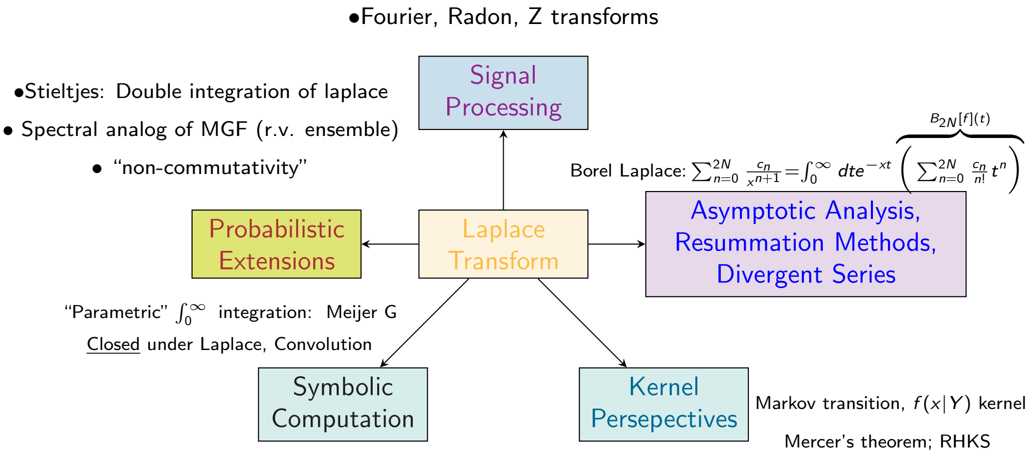

Figure: Laplace transform Landscape

Overview

The pipeline

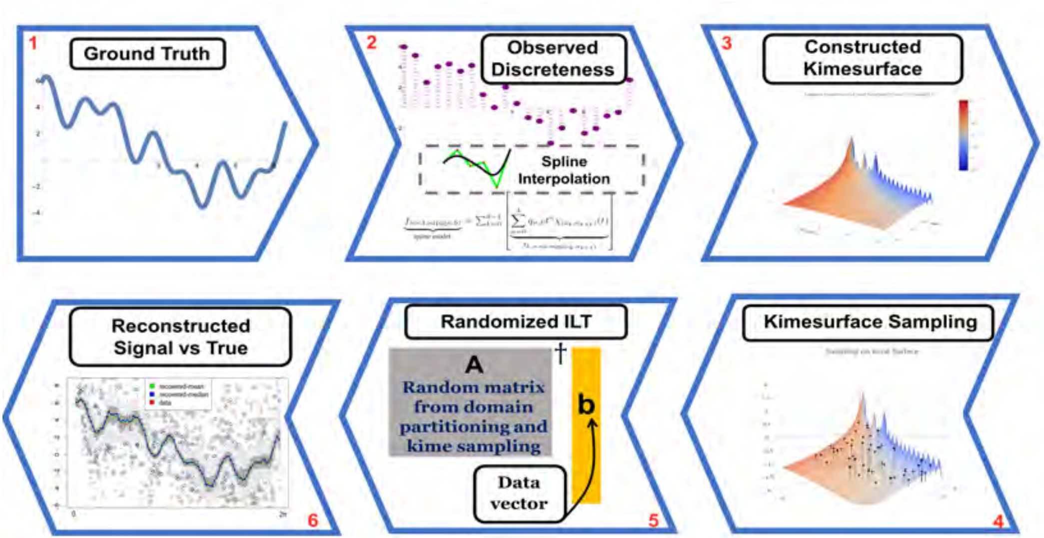

The forward transform

Similar to Borel series expanded as integral representation

$$\sum_{n=0}^{2N} \frac{c_n}{x^{n+1}} = \int_0^{\infty} dt e^{-xt} \underbrace{\left(\sum_{n=0}^{2N} \frac{c_n}{n!} t^n \right)}_{B_{2N}[f](t)} \tag{5}$$

1. For data science application, we care about finite observations $\int_0^{\infty} \Longrightarrow \int_0^{a}$ (or do we say we restrict the analysis to finite observations)
2. We are not considering decoding/modeling singularities, hence N is reasonably small and finite.

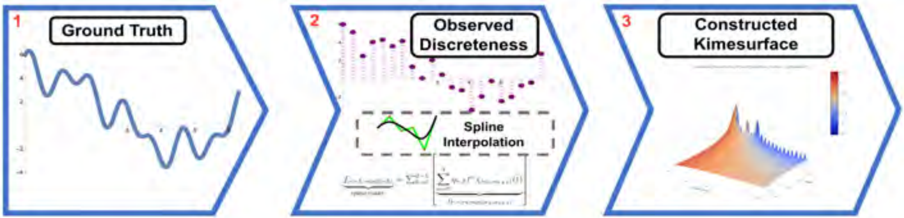

The Inverse transform

Similar to Borel series expanded as integral representation

$$\sum_{n=0}^{2N}\frac{c_n}{x^{n+1}} = \int_0^{\infty} dt e^{-xt}\underbrace{\left(\sum_{n=0}^{2N}\frac{c_n}{n!}t^n\right)}_{B_{2N}[f](t)} \tag{6}$$

1. where LT goes from right to left, ILT goes from left to right
2. Use sampling to gauge the problem of requiring precise functional representation.
3. Thm: Sampling on a surface is sufficient to reconstruct the functional information on an analytic kime surface

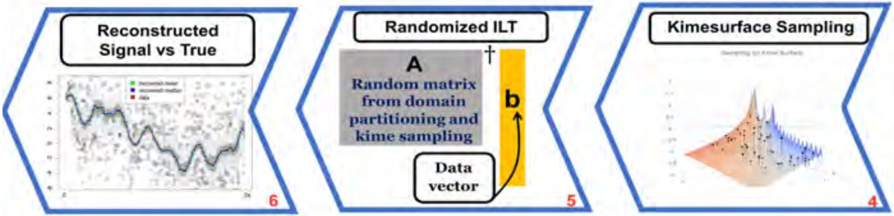

Algorithms and Analysis

Algorithm 1 Randomized ILT

$N_1, N_2 \leftarrow \textit{prior\_estimate}$ is the partition size
$itn \leftarrow g(N_1, N_2, \textit{prior\_estimate})$ is the number of attempts ($\textit{iterations}$)
for $1 \leq k \leq itn$ **do**
  $\mathbf{p}^k \leftarrow$ Random N_1 size partition on interval $(0, 2\pi)$, according to distribution P.
  $\mathbf{b} = (b_i) \leftarrow$ Random N_2 points (z_i, b_i) from the dataset S
  $\mathbf{A} \leftarrow (a_{ij} = \frac{1}{-z_i}(\exp(-z_i p_j) - \exp(-z_i p_{j-1}))$, note that $\mathbf{A}$ is the matrix computing LT of a quantized piecewise constant function
  $\mathbf{u}^{pk} = \mathbf{A}^{-1}\mathbf{b}$
  $f^{pk} \leftarrow \mathbf{u}^{pk}$ as a piecewise constant function
end for
$f \leftarrow \frac{1}{itn}\sum_k f^{pk}$

Unfortunately, the entries of our LT matrix A are far from independent and A may not be Hermitian. Hence, there is little guarantee that direct applications of random matrix theory may ensure reasonable approximations of the smallest singular value of the LT matrix. However, we are able to perform empirical evaluation on this method.

Empirical Results - LT

$$f(x) = 2\sin(x) + \cos(4x) + \sin(7x + 0.5) + (x-3)(x-5) * 0.3 + \varepsilon(x)$$

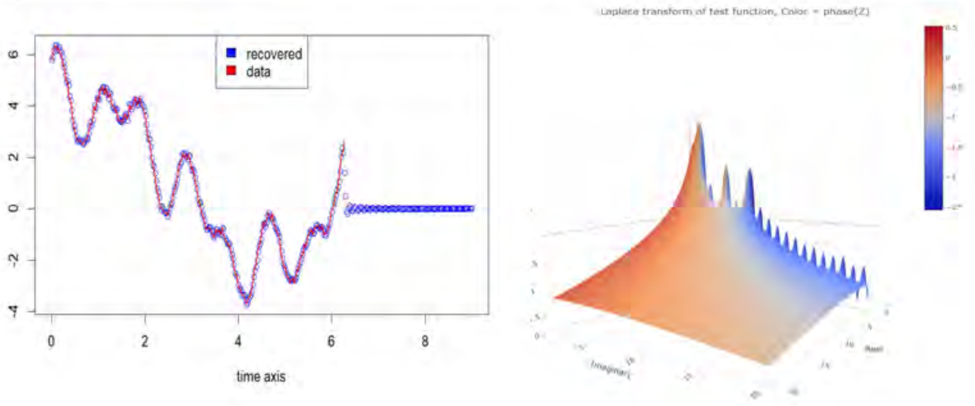

Empirical Result - ILT

$$f(x) = 2\sin(x) + \cos(4x) + \sin(7x + 0.5) + (x - 3)(x - 5) * 0.3 + \varepsilon(x)$$

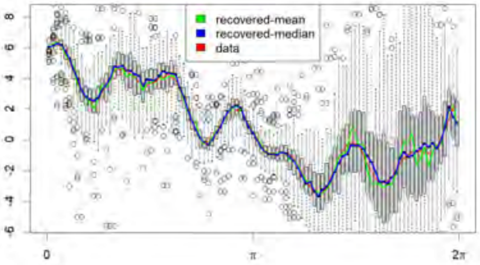

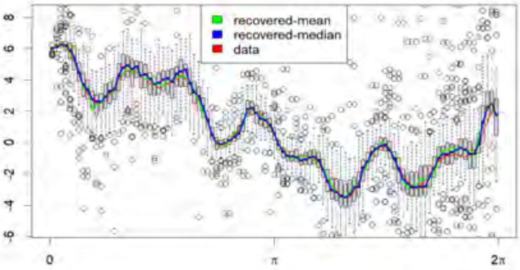

Overview

How does the spline interpolation generalizes for unknown signal?

The error for spline interpolation (i.e., f_{sp} vs f_{true}) is bounded by the maximal sampling distance and a energy norm on the derivative of the signal.

Theorem (1909.03559)

If $u \in H^r(a,b) = \{u \in L^2(a,b) : \partial^\alpha u \in L^2(a,b), \alpha = 1,2,...,r\}$, and $h = \max_{j=0,1,2....N} |x_{j+1} - x_j|$, then

$$\|u - S_p^k u\| \le \min\left\{\left(\frac{eh}{4(p-k)}\right)^r \|\partial^r u\|, (\frac{h}{\pi})^r \|\partial^r u\|\right\} \quad (7)$$

for spline approximants $S_p^k u$ with pth degree and kth smoothnoess.

Deviation between the true surface and the fitted surface?

A straightforward analysis gives a generic but crude bound:

$$\begin{aligned}|F_{d,4}(z)-F_a(z)| &= \left|\int_a^b (f_{n=4,\mathrm{supp}[a,b)}(t)-f(t))e^{-zt}dt\right| \le \int_a^b \sup_{a\le t<b} |f_{4,\mathrm{supp}[a,b)}(t)-f(t)|\cdot|e^{-zt}|dt \\ &= \sup_{a\le t<b} |f_{4,\mathrm{supp}[a,b)}(t)-f(t)| \times \frac{e^{-Re(z)a}-e^{-Re(z)b}}{Re(z)} .\end{aligned} \tag{8}$$

How does the numerical inverse preserve the fidelity?

We start with the heuristic formulation

$$\begin{aligned} F(z_i) &= \int_0^{2\pi} f(t)e^{-zt}dt = \sum_{p_i} \int_{p_{i-1}}^{p_i} f(t)e^{-z_i t}dt \approx \sum_{p_i} f(p_{i-1}) \int_{p_{i-1}}^{p_i} e^{-z_i t}dt \\ &= \sum_{p_i} f(p_{i-1})(-\frac{1}{z_i})\Big[\exp(-z_i p_i) - \exp(-z_i p_{i-1})\Big] \end{aligned} \tag{9}$$

Writing our in matrix form with $a_{ij} = (-\frac{1}{z_i})\Big[\exp(-z_j p_j) - \exp(-z_j p_{j-1})\Big]$

$$\begin{bmatrix} F(z_1) \\ F(z_2) \\ \dots \\ F(z_N) \end{bmatrix} = \underbrace{\begin{bmatrix} a_{11} & a_{12} & a_{13} & \dots & a_{1n} \\ a_{21} & a_{22} & a_{23} & \dots & a_{2n} \\ \dots & \dots & \dots & \dots & \dots \\ a_{N1} & a_{N2} & a_{N3} & \dots & a_{Nn} \end{bmatrix}}_{A} \begin{bmatrix} f(p_1) \\ f(p_2) \\ \dots \\ f(p_n) \end{bmatrix}$$

In essence, we have $\boldsymbol{F} \approx \boldsymbol{Af}$. Our numerical scheme requires a bound for smallest singular value of A ($\|A^\dagger\|_F$): $\|A^\dagger F_{true} - f_{true}\|_2 = \{A^\dagger A = I\} = \|A^\dagger(F_{true} - Af_{true})\|_2 \leq \|A^\dagger\|_F \|F_{true} - Af_{true}\|_2$

Random Matrix results

- If iid entries, mean zero, unit variance assumption is not satisfied. We can try to resort to isotropicity for $A = \left(\frac{1}{-z_i} (\exp(-z_i p_j) - \exp(-z_i p_{j-1})) \right)_{1 \le i \le n', 1 \le j \le n}$

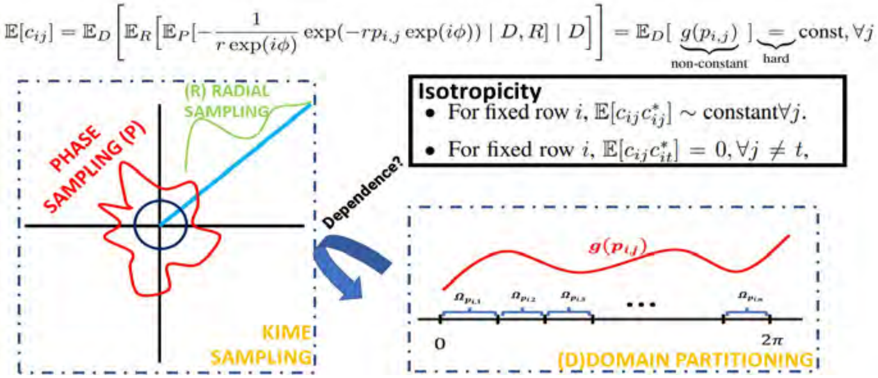

Figure: Intuition: Use randomness "smooth" out the singularity [Limitations and bounds (partial)]:

Overview

Acknowledgement: Collaborators and SOCR team

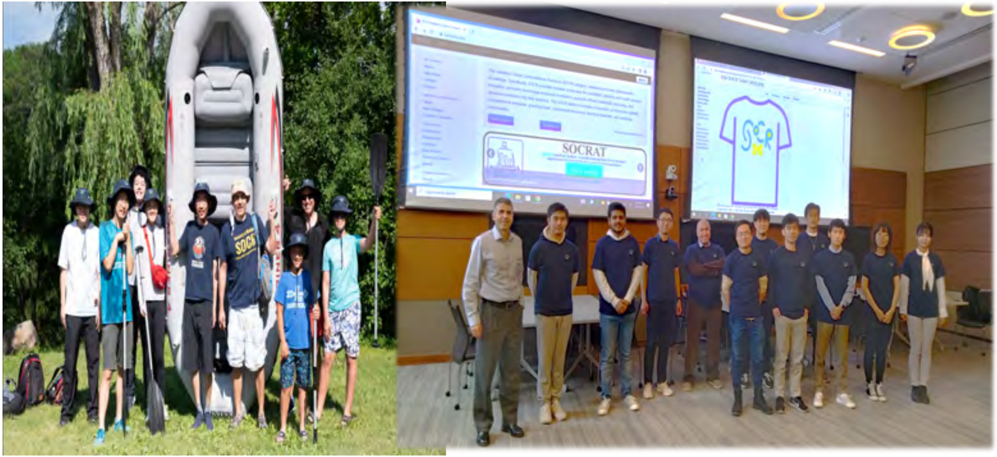

SOCR technologies

- TCIU package: https://cran.r-project.org/web/packages/TCIU/index.html
- Github link: https://github.com/SOCR/TCIU
- SOCR link: https://www.socr.umich.edu/
- TCIU tutorials: https://www.socr.umich.edu/TCIU/

References

[1] Edward Anderson. "Problem of time in quantum gravity". In: *Annalen der Physik* 524.12 (2012), pp. 757–786.

[2] Johannes Brandstetter et al. "Clifford neural layers for PDE modeling". In: *arXiv preprint arXiv:2209.04934* (2022).

[3] Eckhard Hitzer and Stephen J Sangwine. *Quaternion and Clifford Fourier transforms and wavelets*. Springer, 2013.

[4] George W Mackey. "The Laplace transform for locally compact Abelian groups". In: *Proceedings of the National Academy of Sciences* 34.4 (1948), pp. 156–162.

[5] Arakaparampil M Mathai and Ram Kishore Saxena. *Generalized hypergeometric functions with applications in statistics and physical sciences*. Vol. 348. Springer, 2006.

[6] Tyre Newton and Thomas Lofaro. "On using flows to visualize functions of a complex variable". In: *Mathematics Magazine* 69.1 (1996), pp. 28–34.

[7] Fritz Peter and Hermann Weyl. "Die Vollständigkeit der primitiven Darstellungen einer geschlossenen kontinuierlichen Gruppe". In: *Mathematische Annalen* 97.1 (1927), pp. 737–755.

[8] Marc-Olivier Renou et al. "Quantum theory based on real numbers can be experimentally falsified". In: *Nature* 600.7890 (2021), pp. 625–629.

Overview

Transforms on group

The canonical Fourier analysis can be extended to topological groups by virtue of Peter-Weyl's result[4]

$$\begin{aligned} \text{Forward}: \hat{f}(\rho_l) &= [\mathcal{F}_G f]_l = \int_G f(g)\rho_l(g)dg \\ \text{Backward}: \left[\mathcal{F}_G^{-1}\hat{f}\right]_l &= \sum_l d_{\rho_l} tr\left[\hat{f}(\rho_l)\rho_l(g^{-1})\right] \end{aligned} \tag{10}$$

The case of $SO(2)$: $U(1) = S^1 \cong SO(2)$. 1D complex irreps $\rho_l(g \equiv e^{i\theta}) = e^{il\theta}, l \in \mathbb{Z}$ are the circular harmonics. This is the complex Fourier-Euler basis $\{\sqrt{\frac{1}{2\pi}}e^{in\theta}\}_{n=-\infty}^{\infty}$ for 1D Fourier Series for $L^2([0, 2\pi])$.

$$\mathcal{F}_G^{-1}\hat{f} = f(x) = \sum_{l\in\mathbb{Z}} \underbrace{\frac{1}{2\pi}\int_0^{2\pi} f(\theta)e^{il\theta}d\theta}_{\mathcal{F}_G f} \cdot e^{-ilx} \tag{11}$$

- Limited studies have tried to extend this to groups (locally compact Abelian)-Gelfand transform [5].

[4] Fritz Peter and Hermann Weyl. "Die Vollständigkeit der primitiven Darstellungen einer geschlossenen kontinuierlichen Gruppe". In: *Mathematische Annalen* 97.1 (1927), pp. 737–755

[5] George W Mackey. "The Laplace transform for locally compact Abelian groups". In: *Proceedings of the National Academy of Sciences* 34.4 (1948), pp. 156–162

Clifford Algebra

The main motivation is to define Laplace transform for Clifford spacetime algebra. The main challenge for a closed form solution is the BCH condition suggesting non-commutativity:

$$
\begin{aligned}
e^{M_1}e^{M_2} &= e^{M_1+M_2+\frac{1}{2}[M_1,M_2]+\frac{1}{12}([M_1,[M_1,M_2]]+[M_2,[M_2,M_1]])+\dots} \\
e^{M_1}e^{M_2} &\neq e^{M_1+M_2} \text{ for } [M_1, M_2] \neq 0
\end{aligned}
\tag{12}
$$

We may formulate this in a more general framework of geometric algebra (Clifford algebra), where

1. $\mathrm{Cl}_{1,3}(\mathbb{R})$ correspond to the spacetime algebra with metric signature $(+,-,-,-)$
2. $\mathrm{Cl}_{0,2}(\mathbb{R})$. Quarternion ($\mathbb{H} \cong \mathrm{Cl}_{0,2}(\mathbb{R})$)
3. $\mathrm{Cl}_{0,1}(\mathbb{R})$ complex numbers ($\mathbb{C} \cong \mathrm{Cl}_{0,1}(\mathbb{R})$)
4. $\mathrm{Cl}_{0,0}(\mathbb{R})$ real numbers ($\mathbb{R} \cong \mathrm{Cl}_{0,0}(\mathbb{R})$)

Clifford-Fourier Transforms

- The Case for $\mathrm{Cl}_{2,0}(\mathbb{R})$. The vector space G^2 of the algebra contains the basis $\{1, e_1, e_2, e_1e_2\}$. The peculiarity is that $(e_1e_2)^2 = e_1e_2e_1e_2 = -e_1e_2e_2e_1 = -1$. The bivector e_1e_2 is associated with a pseudoscalar (correspond to highest grade basis) $i_2 = e_1e_2, i_2^2 = -1$. The pseudoscalar gives an alternative expression for the basis decomposition $\boldsymbol{f}(x) = f_0 + f_1e_1 + f_2e_2 + f_{12}e_{12} = 1(f_0(x) + f_{12}(x)i_2) + e_1(f_1(x) + f_2(x)i_2)$. In the algebraic constraints, i_2 behaves like the imaginary number i hence the 2D Clifford Fourier transform operates on spinor $(f_0(x) + f_{12}(x)i_2)$ and vector $(f_1(x) + f_2(x)i_2)$ component separately is naturally defined as [6]

$$\hat{\boldsymbol{f}}(\xi) = \mathcal{F}\{\boldsymbol{f}\}(\xi) = \int_{\mathbb{R}^2} \boldsymbol{f}(x)e^{-2\pi i_2\langle x,\xi\rangle}dx, \quad \forall \xi \in \mathbb{R}^2 \tag{13}$$

$$\boldsymbol{f}(x) = \mathcal{F}^{-1}\{\mathcal{F}\{\boldsymbol{f}\}\}(x) = \int_{\mathbb{R}^2} \hat{\boldsymbol{f}}(\xi)e^{2\pi i_2\langle x,\xi\rangle}d\xi, \quad \forall x \in \mathbb{R}^2 \tag{14}$$

[6] Johannes Brandstetter et al. "Clifford neural layers for PDE modeling". In: *arXiv preprint arXiv:2209.04934* (2022).

Clifford Fourier Transform

- The Case for $\mathrm{Cl}_{0,2}(\mathbb{R})$. Quarternion ($\mathbb{H} \cong \mathrm{Cl}_{0,2}(\mathbb{R})$)The Clifford Fourier transform [7]

$$\mathcal{F}^{cl}\{f\}(\underbrace{u_1, u_2}_{\boldsymbol{u}}) = \int_{\mathbb{R}^2} f(\boldsymbol{x}) e^{-2\pi e_1 u_1 x_1} e^{-2\pi e_2 u_2 x_2} d\boldsymbol{x} \tag{15}$$

$$f(\boldsymbol{x}) = (\mathcal{F}^{-1})^{cl}\{\hat{f}\}(\boldsymbol{x}) = \int_{\mathbb{R}^2} \hat{f}(\boldsymbol{u}) e^{2\pi e_2 x_2 u_2} e^{2\pi e_1 x_1 u_1} d\boldsymbol{u} \tag{16}$$

The more specialized transform for quaternions is to sandwiching the function using exponentials

$$\mathcal{F}^{q}\{f\}(\underbrace{u_1, u_2}_{\boldsymbol{u}}) = \int_{\mathbb{R}^2} e^{-2\pi e_1 u_1 x_1} f(\boldsymbol{x}) e^{-2\pi e_2 u_2 x_2} d\boldsymbol{x} \tag{17}$$

$$f(\boldsymbol{x}) = (\mathcal{F}^{-1})^{q}\{\hat{f}\}(\boldsymbol{x}) = \int_{\mathbb{R}^2} e^{2\pi e_1 x_1 u_1} \hat{f}(\boldsymbol{u}) e^{2\pi e_2 x_2 u_2} d\boldsymbol{u} \tag{18}$$

where $e_1 = \hat{\boldsymbol{i}}, e_2 = \hat{\boldsymbol{j}}, e_1 e_2 = \hat{\boldsymbol{i}}\hat{\boldsymbol{j}} = \hat{\boldsymbol{k}}$.

[7] Eckhard Hitzer and Stephen J Sangwine. *Quaternion and Clifford Fourier transforms and wavelets.* Springer, 2013.

Clifford Fourier Transform

- The Case for spacetime algebra $\mathrm{Cl}_{3,1}(\mathbb{R})$. We can extend the defintion to complex signatures and obtaining transforms for spacetime algebras utilizing the pseudoscalars and quarternion fourier transform definition with east coast metric signature $(+,+,+,-)$ [8]

$$\hat{f}(\boldsymbol{u}) = \mathcal{F}\{f\}(\boldsymbol{u}) = \int_{\mathbb{R}^{3,1}} e^{-2\pi e_0 ts} f(\boldsymbol{x}) e^{-2\pi i_3 \langle x,u \rangle} d^4\boldsymbol{x} \tag{19}$$

$$f(\boldsymbol{x}) = (\mathcal{F}^{-1})\{\hat{f}\}(\boldsymbol{x}) = \int_{\mathbb{R}^{3,1}} e^{2\pi e_0 ts} \hat{f}(\boldsymbol{u}) e^{2\pi i_3 \langle x,u \rangle} d^4\boldsymbol{u} \tag{20}$$

where $f : \mathbb{R}^{3,1} \to \mathrm{Cl}_{3,1}(\mathbb{R})$, and i_3 is the pseudo-scalar in $\mathrm{Cl}_{3,0}(\mathbb{R})$, where the spacetime vectors and spacetime frequency are defined by $\boldsymbol{x} = te_0 + x, x = x_1 e_1 + x_2 e_2 + x_3 e_3$ and $\boldsymbol{u} = se_0 + u, u = u_1 e_1 + u_2 e_2 + u_3 e_3$ respectively.

[8] Eckhard Hitzer and Stephen J Sangwine. *Quaternion and Clifford Fourier transforms and wavelets.* Springer, 2013

Closure and Invertibility

Closure$\Longrightarrow$Universality

Invertibility functional examples:

1. $\underbrace{\text{Squared integrable functions}}_{L^2([0,\infty))} \Longleftrightarrow \underbrace{\text{Hardy space}}_{H(\mathbb{C}_+)}$,
2. resurgent functions $\Longleftrightarrow$ resurgent series[9]

Closure properties

1. The Laplace transform of a Meijer G function is also Meijer G function
2. The Laplace transform of resurgent function is also resurgent[9].

[9] https://online.kitp.ucsb.edu/online/resurgent-c17/costin/pdf/Costin_Resurgent17Conf_KITP.pdf

Visualizations

- Kimesurfaces features: ▶ Monotonicity dampens the oscillation in magnitude ▶Periodicity translates to more oscillations on the magnitude

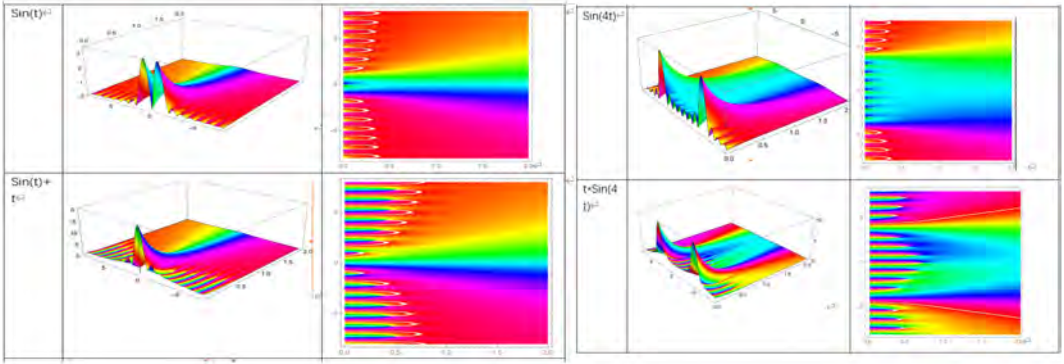

Figure: Kimesurface features

The principal Kime Domain Motivation: Riemann Mapping theorem

1. Riemann Mapping theorem. (proper, simply connected, non-empty open subset U of $\mathbb{C}$ is conformally equivalent to the open unit disk D^2). This hints the open unit disk representation is fundamental

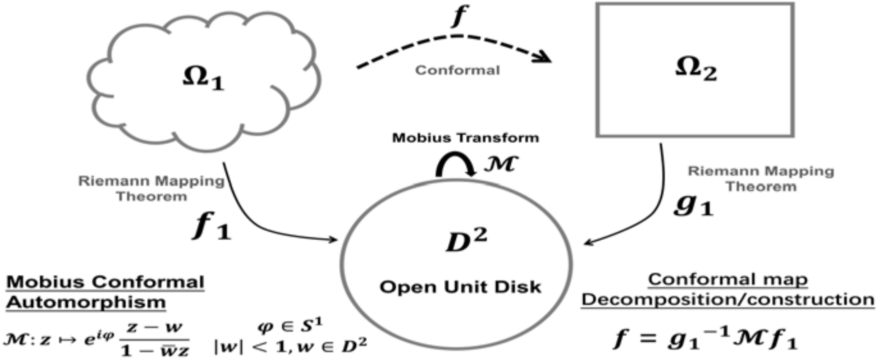

Figure: Mapping theorem

The principal Kime Domain Motivation 2: Algebraic Calculation Example

1. Example 1: Consider the numerical evaluation of $\left(e^{2\pi i}\right)^{2\pi i}$. On one hand, this is
   - $\left(e^{2\pi i}\right)^{2\pi i} = 1^{2\pi i} = 1$

   On the other hand, this is
   - $\left(e^{2\pi i}\right)^{2\pi i} = e^{-4\pi^2} \neq 1$
2. Example 2: Consider the numerical evaluation of $\left((-1)\cdot(-1)\right)^{-i}$. On one hand, this is
   - $\left((-1)\cdot(-1)\right)^{-i} = (1)^{-i} = 1$

   On the other hand, this is
   - $(e^{\pi i} \cdot e^{\pi i})^{-i} = e^{\pi} \cdot e^{\pi} = e^{2\pi} = 535.49$
3. The problem underlying this numerical catastrophe is the fact that $(z_1 z_2)^a = z_1^a z_2^a$, $(e^{z_1})^{z_2} = e^{z_1 z_2}$ does not hold.
   - ▶ The root cause is that logarithm $ln(z)$ is multivalued
4. (Partial) Resolution: defining the principal value (phase) $Arg(z)$: $-\pi < Arg(z) \leq \pi$ $ln(z) = Ln|z| + iArg(z) + 2\pi iN$, $N = 0, \pm 1, \pm 2, \ldots$, and perform the calculations carefully.

The principal Kime Domain Motivation 2: Algebraic Calculation Example (contd)

Insisting the principal value (phase) $-\pi < Arg(z) \leq \pi$

1. Example 1: Consider the numerical evaluation of $\left(e^{2\pi i}\right)^{2\pi i}$.
   - $\left(e^{2\pi i}\right)^{2\pi i} = \{z^a = e^{a ln(z)}\} = e^{2\pi i \left(ln(e^{2\pi i})\right)} \underbrace{=}_{\text{principal value: } ln(e^{2\pi i})=0} e^0 = 1$
     - If we do not insist on the principal value, then $ln(e^{2\pi i}) = 2\pi i$, hence $\left(e^{2\pi i}\right)^{2\pi i} = e^{2\pi i \times 2\pi i} = e^{-4\pi^2}$
2. Example 2: Consider the numerical evaluation of $\left((-1)\cdot(-1)\right)^{-i}$.
   - $\left((-1)\cdot(-1)\right)^{-i} = \{z^a = e^{a ln(z)}\} = e^{-i\cdot(ln((-1)\cdot(-1)))} = e^{-i\cdot 0} = 1$
     - The problem with the original approach is that $ln((-1)\cdot(-1)) = ln(-1) + ln(-1) = \pm 2\pi i$, but insisting on the principal value the result should be 0 all along (or the final calculation quantity should mod $2\pi i$ so that $-\pi < |Arg(ln((-1)\cdot(-1)))| \leq \pi$).

For general abstract formula (See http://scipp.ucsc.edu/~haber/ph116A/clog_11.pdf)

The principal Kime Domain Motivation 3 : Dealing with singularities after the conformal map is more numerically stable

Branchpoints (It turns out dealing with branch points can be much more effectively dealt with if one first conformally mapped to a disk and then perform Padé and then transform back (2208.02410).)

1. Numerical strategies may be more effective in this domain after applying riemann mapping.

Laplace transforms - Preliminaries

- The Laplace transform is a **bounded** linear map - by defining $\mathcal{L} : L^2([0,\infty)) \to H^2(\mathbb{C}_+)$, $\|\mathcal{L}f\|_{H^2}(\mathbb{C}_+) = \|f\|_{L^2([0,\infty))}$

Laplace transforms - Preliminaries

- The Laplace transform is a **bounded** linear map - by defining $\mathcal{L} : L^2([0,\infty)) \to H^2(\mathbb{C}_+)$, $\|\mathcal{L}f\|_{H^2}(\mathbb{C}_+) = \|f\|_{L^2([0,\infty))}$
  - The invertibility in this class of function is given by the Bromwhich integral

$$\mathcal{L}^{-1}\{F(s)\} = \frac{1}{2\pi i}\int_{-i\infty}^{i\infty} F(s)e^{st}\,ds$$

Laplace transforms - Preliminaries

- The Laplace transform is a **bounded** linear map - by defining $\mathcal{L} : L^2([0,\infty)) \to H^2(\mathbb{C}_+)$, $\|\mathcal{L}f\|_{H^2(\mathbb{C}_+)} = \|f\|_{L^2([0,\infty))}$
  - The invertibility in this class of function is given by the Bromwhich integral

$$\mathcal{L}^{-1}\{F(s)\} = \frac{1}{2\pi i}\int_{-i\infty}^{i\infty} F(s)e^{st}ds$$

  - The general Bromwhich condition is introduced with the decay factor γ such that $e^{-\gamma t}f \in L^2([0,\infty))$

$$\mathcal{L}^{-1}\{F(s)\} = \frac{1}{2\pi i}\int_{\gamma-i\infty}^{\gamma+i\infty} F(s)e^{st}ds$$

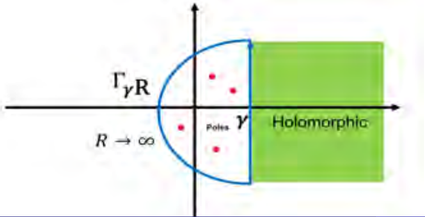

Laplace transforms - Preliminaries

- The Laplace transform is a **bounded** linear map - by defining $\mathcal{L} : L^2([0,\infty)) \to H^2(\mathbb{C}_+)$, $\|\mathcal{L}f\|_{H^2(\mathbb{C}_+)} = \|f\|_{L^2([0,\infty))}$
  - ▶ The general Bromwhich condition is introduced with the decay factor γ such that $e^{-\gamma t} f \in L^2([0,\infty))$

$$\mathcal{L}^{-1}\{F(s)\} = \frac{1}{2\pi i}\int_{\gamma - i\infty}^{\gamma + i\infty} F(s) e^{st} ds$$

  - ▶ The general functional assumption in real life is often intractable. If the function is in the class then we expect to get sensible results for approximation error.

Laplace transforms - Preliminaries

- The Laplace transform is a **bounded** linear map - by defining $\mathcal{L} : L^2([0,\infty)) \to H^2(\mathbb{C}_+)$, $\|\mathcal{L}f\|_{H^2(\mathbb{C}_+)} = \|f\|_{L^2([0,\infty))}$
  - The general Bromwhich condition is introduced with the decay factor γ such that $e^{-\gamma t}f \in L^2([0,\infty))$

$$\mathcal{L}^{-1}\{F(s)\} = \frac{1}{2\pi i}\int_{\gamma-i\infty}^{\gamma+i\infty} F(s)e^{st}ds$$

  - The general functional assumption in real life is often intractable. If the function is in the class then we expect to get sensible results for approximation error.
- Laplace transform facilitates the **calculation of moments**. It has a nice connection with moment generating function $X \geq 0$. Using the Laplace transform, we can recover the cumulative distribution function, F_X, of a continuous random variable X.

- The Laplace transform is a **bounded** linear map - by defining $\mathcal{L}: L^2([0,\infty)) \to H^2(\mathbb{C}_+)$, $\|\mathcal{L}f\|_{H^2}(\mathbb{C}_+) = \|f\|_{L^2([0,\infty))}$
  - The general Bromwhich condition is introduced with the decay factor γ such that $e^{-\gamma t} f \in L^2([0,\infty))$

$$\mathcal{L}^{-1}\{F(s)\} = \frac{1}{2\pi i}\int_{\gamma - i\infty}^{\gamma + i\infty} F(s) e^{st} ds$$

  - The general functional assumption in real life is often intractable. If the function is in the class then we expect to get sensible results for approximation error.
- Laplace transform facilitates the **calculation of moments**. It has a nice connection with moment generating function $X \geq 0$. Using the Laplace transform, we can recover the cumulative distribution function, F_X, of a continuous random variable X.

$$\mathcal{L}\{F_X'\}(x) = \underbrace{F(0)}_{0} + s\mathcal{L}\{F_X\}(x) \Longrightarrow \boxed{F_X(x) = \mathcal{L}^{-1}\left\{\frac{1}{s}\mathbb{E}\left[e^{-sX}\right]\right\}(x) = \mathcal{L}^{-1}\left\{\frac{1}{s}\mathcal{L}\{f_X\}(s)\right\}(x).} \tag{21}$$

Meijer-G function approach

Integral of the product of two Meijer-G functions is another Meijer-G function [10]

$$\int_0^\infty x^{\sigma-1} G^{m,n}_{p,q}\left(wx \,\middle|\, \begin{matrix} a_p \\ b_q \end{matrix}\right) G^{\alpha,\beta}_{\gamma,\delta}\left(\eta x^{k/\rho} \,\middle|\, \begin{matrix} c_\gamma \\ d_\delta \end{matrix}\right) dx$$

$$= C_1 \cdot G^{\rho\alpha+kn,\rho\beta+km}_{\rho\gamma+kq,\rho\delta+k\rho}\left(\frac{\eta^\rho \rho^{\rho(\gamma-\delta)}}{w^k k^{k(p-q)}} \,\middle|\, \begin{matrix} \overbrace{\Delta(\rho,c_1),\ldots,\Delta(\rho,c_\beta),\Delta(k,1-b_1-\sigma),\ldots\Delta(k,1-b_m-\sigma)}^{\beta\rho+km}; \\ \underbrace{\Delta(\rho,d_1),\ldots,\Delta(\rho,d_\alpha),\Delta(k,1-a_1-\sigma),\ldots\Delta(k,1-a_n-\sigma)}_{\rho\alpha+kn}; \end{matrix}\right.$$

$$\left.\begin{matrix} \overbrace{\Delta(k,1-b_{m+1}-\sigma),\ldots,\Delta(k,1-b_q-\sigma),\Delta(\rho,c_{\beta+1}),\ldots,\Delta(\rho,c_\gamma)}^{\rho(\gamma-\beta)+k(q-m)} \\ \underbrace{\Delta(k,1-a_{n+1}-\sigma),\ldots,\Delta(k,1-a_p-\sigma),\Delta(\rho,c_{\alpha+1}),\ldots,\Delta(\rho,c_\delta)}_{\rho(\delta-\alpha)+k(p-n)} \end{matrix}\right),$$

$$C_1 = w^{-\sigma} \rho^{1+\frac{1}{2}(\delta-\gamma)+\sum_{j=1}^{\gamma} c_j - \sum_{j=1}^{\delta} d_j} k^{\sigma(p-q)+\frac{1}{2}(q-p)+\sum_{j=1}^{p} a_j - \sum_{j=1}^{q} b_j} (2\pi)^{\frac{\rho-1}{2}(2\alpha+2\beta-\gamma-\delta)} (2\pi)^{\frac{k-1}{2}(2m+2n-p-q)} \tag{22}$$

[10] Arakaparampil M Mathai and Ram Kishore Saxena. *Generalized hypergeometric functions with applications in statistics and physical sciences*. Vol. 348. Springer, 2006

Meijer G function contd

and the notation $\Delta(\cdot,\cdot)$ is a short hand for a set of indexing argument in the Meijer-G function. For example, $\Delta(\rho, c_j) = \{\frac{c_j+1}{\rho}, \frac{c_j+2}{\rho}, \ldots, \frac{c_j+\rho-1}{\rho}\}$, and the indices by default are non-negative integers. The complete proof for the Meijer-G function property is given in (manuscript). As a corollary, we can derive from the general form for laplace transform

$$\boxed{\int_0^\infty e^{-wx} G^{\alpha,\beta}_{\gamma,\delta}\left(\eta x \middle| \begin{matrix} c_\gamma \\ d_\delta \end{matrix}\right) dx = \frac{1}{w} G^{\alpha,\beta+1}_{\gamma+1,\delta}\left(\frac{\eta}{w} \middle| \begin{matrix} 0, c_\gamma \\ d_\delta \end{matrix}\right).} \tag{23}$$

This would be useful if we can fit using certain Meijer "basis" parametrically (symbolic regression), then then laplace transform is <u>pure symbolic manipulations</u>. Furthermore,

- The forward and inverse laplace transform can be evaluated <u>closed form</u> (given we have robust algorithm for Meijer G function representation).

Limitations for isotropicity

Lemma

(B_{ij} sampling) Given that ϕ and a (the radial sampling, and the domain partitioning altogether is resembled by a) are independent, i.e., the sampling scheme, kime phase, and kime magnitude (radial) sampling processes are independent, then the only $f_\Phi(\phi) \in L^2([0, 2\pi])$ such that

$$\int_0^{2\pi} \exp(-a \exp(i\phi)) f_\Phi(\phi) d\phi = const, \tag{24}$$

is $f_\Phi(\phi) = \frac{1}{2\pi}$. With $B = \left((\exp(-z_i p_j) - \exp(-z_i p_{j-1}))\right)_{1 \le i \le n', 1 \le j \le n}$

Limitation contd

Lemma

(A_{ij} sampling) If a and ϕ are independent (meaning that the phase sampling is independent of the radial direction and the domain partitioning), then there exists no square-integrable function $f_\Phi(\phi)$, such that

$$\int_0^{2\pi} \exp(a\exp(i\phi))\exp(-i\phi)f_\Phi(\phi)d\phi = const \quad (25)$$

where the constant is independent of a.

A possible strategy

Consider the following von Mises distribution

$$f_\Phi(\phi) = \frac{\exp(-a\cos(\phi))}{2\pi I_0(a)} \tag{26}$$

and the following two integrals

$$\mathbb{E}[c_{ij}] = \int_0^{2\pi} \exp(ae^{i\phi}) f_\Phi(\phi) d\phi = \frac{2\pi J_0(a)}{2\pi I_0(a)} = \frac{J_0(a)}{I_0(a)} \tag{27}$$

$$\mathbb{E}[c_{ij}c_{ij}^*] = \int_0^{2\pi} \exp(ae^{i\phi}) \exp(ae^{i\phi})^* f_\Phi(\phi) d\phi = \int_0^{2\pi} \exp(2a\cos\phi) \frac{\exp(-a\cos(\phi))}{2\pi I_0(a)} d\phi = 1. \tag{28}$$

Therefore, if we focus on the zeros of the Bessel functions of the 0^{th}-kind, $J_0(a)$, we can guarantee isotropicity. The numerical algorithm roughly goes the following:

- Use r (radial component) as a scaling parameter so that we have enough zeros from $[0,2\pi]$ to fit in the zeros such that $J_0(r \cdot p_{i,j}) = 0$ deterministically for $p_{i,j}$.
- Then at each entry sample the phase according to the distribution $f_\Phi(\phi) = \frac{\exp(-r \cdot p_{i,j}\cos(\phi))}{2\pi I_0(r \cdot p_{i,j})}$, then the vectors are isotropic, hence singular values of $C_{ij} = \exp(-z_i p_{i,j}), j = 1, 2, 3, \ldots n+1$ are bounded.